Available online at www.sciencedirect.com

ScienceDirect

Energy Procedia 49 (2014) 386 – 397

Energy Procedia

SolarPACES 2013

Linear Fresnel collector receiver: heat loss and temperatures

A. Heimsath[a,*], F. Cuevas[a], A. Hofer[a], P. Nitz[a], W.J. Platzer[a]

[a]*Fraunhofer Institute for Solar Energy Systems, Devisiont Solar Thermal and Optics, Heidenhofstraße 2, 79110 Freiburg, Germany*

Abstract

For design and component specification of a Linear Fresnel Collector (LFC) cavity receiver, the prediction of temperature distribution and heat loss is of great importance. In this paper we present a sensitivity analysis for a range of geometry and material parameters. For the LFC receiver analysis we use two models developed at Fraunhofer ISE. One is a detailed model, combining the spatial distribution of reflected radiation via ray tracing with detailed convective simulations through computational fluid dynamics. The second one is a fast algorithm based on a thermal resistance model. It is applying a similar methodology as the well-known model for vacuum absorber, enhancing an absorber tube model by parameters describing the influence of the secondary mirror and cover glass. The thermal resistance model is described in detail. Obtained results indicate a significant effect of the secondary mirror temperature on heat loss for specific geometries.

Selection and peer review by the scientific conference committee of SolarPACES 2013 under responsibility of PSE AG.
Final manuscript published as received without editorial corrections.
Keywords: Linear Fresnel collector; cavity receiver; heat loss; thermal model

1. Introduction

The Linear Fresnel Collector (LFC) is a line focusing concentrating collector suitable for solar thermal power generation and production of process heat. Direct solar irradiation is reflected onto a stationary receiver by a primary mirror field, consisting of an array of elastically bent mirrors. For the reduction of optical losses, a secondary mirror is positioned above the absorber tube. This unit consisting of absorber tube, optional glass covers and secondary mirror is called the (cavity) receiver of the LFC (see Fig.1). The LFC is a linear concentrating collector, like the well-established Parabolic Trough Collectors (PTC), for which standard optical and thermal models exist. The

* Corresponding author. Tel.: +49-761-4588-5944; fax: +49-761-4588-9410.
E-mail address: anna.heimsath@ise.fraunhofer.de

Selection and peer review by the scientific conference committee of SolarPACES 2013 under responsibility of PSE AG.
Final manuscript published as received without editorial corrections.
doi:10.1016/j.egypro.2014.03.042

investigation in the present paper describes the extension of standard PTC thermal models to be applied for LFC, which leads to more accurate performance prediction. The models predict temperature distribution and heat loss, which are especially relevant for the design and optimization of a receiver. The estimation of heat loss is of importance because the receiver design, like the distance between secondary mirrors and absorber tube as well as the absorber size, is defined by a trade-off between optical and thermal loss. Additionally, the temperature distribution on the secondary mirror and absorber tube are of significance, because the predicted maximum temperature on the secondary is a limiting design factor due to material stability. The temperature influences the heat loss as well. That is why by means of the incorporated models, temperatures on the secondary can be predicted and the influences of the thermal behavior of the cavity receiver on the overall heat loss are estimated.

Nomenclature

DNI	Direct Normal Irradiance (W m^{-2})
$\dot{q}_{x\_y\_cond}$	conductive heat flow from surface x to surface y of cavity receiver (W m^{-1})
$\dot{q}_{x\_y\_conv}$	convective heat flow from surface x to surface y of cavity receiver (W m^{-1})
$\dot{q}_{x\_y\_rad}$	heat flow via radiation from surface x to surface y of cavity receiver (W m^{-1})
$\dot{q}_{x\_SolAbs}$	absorbed solar radiation by surface x (W m^{-1})
Th / θ	angle of incidence of solar radiation (°)
Abbreviations	
Abs_rad	absorbed radiation of secondary mirror
CFD	Computer Fluid Dynamics
Conv	convection
CPC	Compound Parabolic Concentrator
Diam	diameter of absorber
Emiss	emittance of the absorber tube
fvDOM	finite volume Discrete Ordinate Method
ISE	Fraunhofer Institute for Solar Energy Systems
LFC	Linear Fresnel Collector
NREL	National Renewable Energy Laboratory
PTC	Parabolic Trough Collector
Rad	radiation
RAS	Reynolds-Averaged Stress
SolAbs	absorbed solar radiation
TRM	Thermal Resistance Model
VDI	Verein Deutscher Ingenieure
Subscripts	
0	normal angle of incidence
abs	outer absorber tube
sec	secondary mirror
t	transversal angle of incidence

For the prediction of temperatures in the receiver we developed a model combining the spatial distribution of radiation reflected by the primary mirrors via ray tracing with detailed convective simulations through computational fluid dynamics. The model is described in section 2.2. For analysis of the general behavior as well as for parameter studies we set up a simplified thermal resistance model (TRM). The TRM is applying a methodology similar to the well-known model for vacuum absorber presented by Forristall [1]. The TRM is describing the heat transfer for an absorber enhanced by parameters for air stable absorber and correlations which describe the influence of a secondary

mirror and glass cover (circular or flat). A thorough description of the TRM for the case of an air receiver with flat cover glass is given in 2.3. The results in section 3 are generated with the CFD and the energy balance model. All exemplary results in this paper refer to the configuration with an air stable receiver and a flat glass cover, see Fig. 1a. The models are, however, applicable to other geometries as well.

1.1. Linear Fresnel collector receiver

The cavity receiver of a LFC consists of an absorber tube and a secondary concentrator. To reduce heat loss the absorber is usually either protected with a glass tube (compare Fig. 1b) or the bottom of the cavity is covered with a glass plate (compare Fig. 1a). An absorber with glass tube may be evacuated, e.g. using a standard vacuum receiver tube originally developed for PTC. A third possibility is to apply a non-evacuated glass tube around an absorber pipe with an air stable coating. The primary mirror field reflects the direct normal radiation into the cavity and due to astigmatism and optical inaccuracies only part of the reflected radiation is hitting the absorber directly. A fraction of the radiation interacts with the secondary reflector and is redirected onto the absorber (see Fig. 2). Since reflection by the secondary is not loss-less, a component of the short wavelength radiation is absorbed by the secondary reflector, increasing its temperature. While the absorber is being heated, it loses heat by long wavelength radiation and convection to the surroundings.

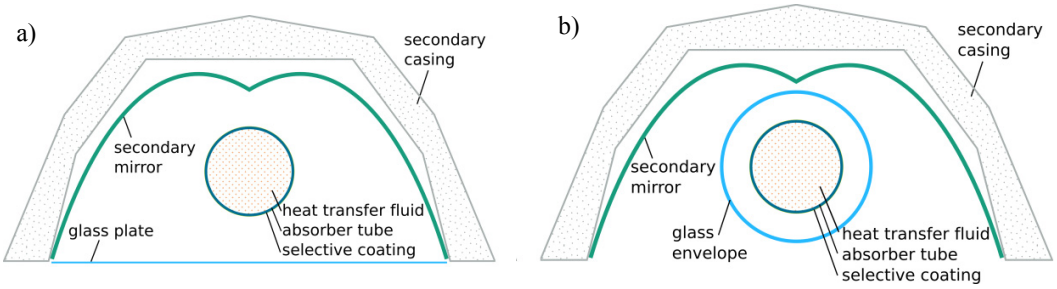

Fig. 1. (a) Sketch of an LFC- receiver with an absorber tube with air stable coating, secondary receiver and glass plate in the bottom; (b) Sketch of LFC-receiver with an absorber tube surrounded by glass envelope; the glass envelope may be evacuated.

2. LFC receiver models

2.1. Optical modeling – ray tracing

For determining the absorbed radiation by the secondary concentrator we use the in-house ray tracing tool Raytrace3D. A set of tools have been developed for the optical modeling and optimization of Linear Fresnel Collector systems [2], Parabolic Trough Collectors, Heliostat Fields [3] and solar Dishes [4]. Raytrace3D is a ray tracing engine designed for solar concentration applications. Furthermore, the ray tracer is integrated together with other optical, technical and economic component simulation models into a powerful multi-parameter design and optimization package for solar thermal power plants [5]. FresnelArray is the tool for the establishment and analysis of geometrical models of Fresnel concentrators. Given a sun position, the inclination of the primary field mirrors is calculated. The rays coming from the light source are reflected by the primary field, losing part of its energy by absorption or scatter. Some rays do not reach the receiver due to blocking and shading between neighboring mirrors. The reflected rays are then transmitted by the glass cover, where part of the ray's energy is lost by absorption and reflection. Some rays directly hit the absorber tube, the remaining rays interact with the secondary reflector and are directed towards the absorber or out of the receiver domain. Fig. 2 shows the interaction of the rays with different surfaces of the receiver. Part of the energy incident on the secondary mirror is absorbed, increasing its temperature.

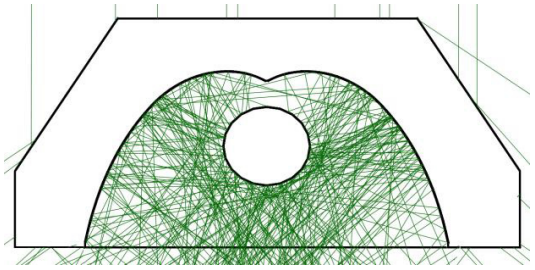

Fig. 2. Ray tracing model of a LFC receiver (visualisation with reduced number of rays). On the top section of the secondary mirror only a small amount of radiation is incident and thus absorbed by the secondary, this section is mostly blocked by the absorber tube. A larger fraction of the radiation hits the reflector in the middle section, leading to absorption and a rise of temperature.

Associating the absorbed radiation with a Direct Normal Incident (DNI) radiation value and a reflective area of the primary field, the absorbed heat flux by the secondary is determined. Fig. 3a shows the geometry of a secondary reflector in the first axis and the absorbed heat flux in the second axis. Three main areas are found with regard to the absorbed flux over the secondary mirror. On the top section of the secondary mirror there is a small amount of absorbed radiation, as this section is blocked by the absorbed tube. On the middle section there is a peak of the flux. In our exemplary calculation reaching values of about 3000 W/m^2. In the lower section the absorbed flux decreases considerably, up to values similar to the ones observed on the top section. Integrating the heat flux over the area of the secondary mirror, the total amount of absorbed radiation is calculated. In the example of Fig. 3a, considering a DNI of 1000 W/m^2 over a primary field area of 12 m^2, a total amount of 600 W is absorbed by the secondary reflector (per meter length of collector). The amount of absorbed radiation is decreasing with the increase of the transversal angle of incidence θ_t. With larger transversal angles the amount of radiation not evenly distributed between the right and the left wing of the secondary reflector increases (see Fig. 3b). However, except for very large transversal angles, the flux is approximately symmetrical.

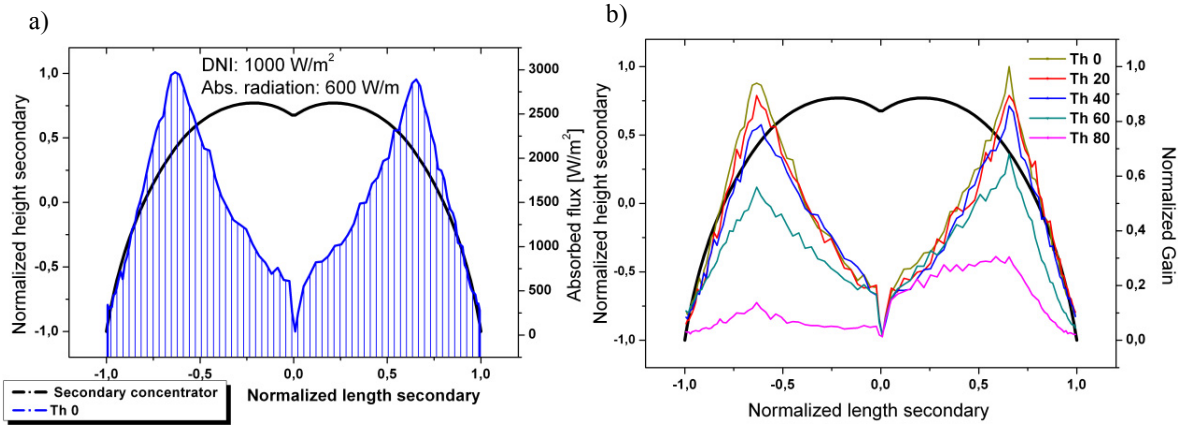

Fig. 3. (a) Result from ray tracing of the absorbed heat flux (blue) for normal incidence and a DNI of 1000 W/m², the shape of the secondary mirror is indicated by the black line. (b) With an increase of the transversal angle of incidence, the interaction with the secondary mirror decreases. The normal angle of incidence is θ_0, quite significant angles for solar positions in southern Europe are around θ_{20} and θ_{40}.

2.2. CFD model

As there is no standard convection correlation for a tube inside a cavity with a non-uniform wall temperature, the open source computer fluid dynamics (CFD) tool OpenFOAM is used, which solves the Navier-Stokes equations by finite volume method. The model considers compressibility of the fluid to take into account the density-temperature dependency. Long wavelength radiation is calculated using the fvDOM model [6]. Short wavelength radiation

absorbed by the secondary concentrator is added as a source-term in the energy equation. The space-resolved quantity of absorbed radiation is generated by ray tracing, see section 2.1.

The scope of the simulation is to determine the heat loss of the receiver and the temperature distribution over the surrounding surfaces. A simulation is performed for a fixed wall temperature of the absorber tube. The secondary concentrator and the glass plate are defined as walls. Proper boundary conditions of the temperature field are defined to consider material properties and ambient conditions. The radiation transport is solved only between boundary surfaces. For every surface the emissivity is set and, given the temperature values of the thermal balance, radiation exchange is calculated. For convection transport, the thermo-physical properties of air are set. The turbulence is simulated with the Reynolds-averaged stress (RAS) model [7]. For exemplary result of the CFD model, see Fig. 7.

2.3. Heat transfer thermal resistance model(TRM)

The model currently developed at Fraunhofer ISE is solving a net of energy balances and heat transfer equations. It is based on extending the heat transfer analysis described by Forristall [1]. Whereas in the NREL-report of Forristall a parabolic trough solar receiver is modeled, the model proposed in this paper expands to a heat loss model for the receiver geometries of Linear Fresnel Collectors, taking into account the thermal balance of the secondary mirror. Figure 4 demonstrates the considered heat flux terms between the different components of a LFC receiver. Heat transports through conduction, convection and radiation as well as the absorbed solar radiation have been implemented in terms of a thermal resistance model (see Fig. 4). Effects of conduction and convection are calculated by physical equations according to VDI Heat Atlas [8]. For the specific geometry of a CPC-like secondary reflector, adapted correlations of similar geometries have been embedded, whose results have been compared with CFD simulations to verify the level of accuracy. Radiation within the cavity of the receiver has been implemented via a view factor model. By means of the open-source software View3d [9]; and taking into account the exact geometry and shape of the secondary mirror, glass plate and absorber a matrix of view factors is generated, that is read in by the simulation environment. Apart from radiation, free convection is considered within the cavity of the receiver. Opposed to the detailed CFD model a homogeneous distribution of the solar radiation on the secondary is implemented. The value implemented corresponds to the total heat absorbed, calculated by ray tracing simulations, as explained in section 2.1. The whole thermal balance is considering a single mean temperature value for the secondary mirror surface. Absorption of the non-reflected solar radiation on the secondary mirror is included in the thermal balance in dependence of the aperture area of the collector, the direct normal irradiance and incidence angle of the solar radiation. Heat transfer to the outer surroundings is characterized by incorporating ambient temperature, wind speed and wind direction. The model was developed for the two general receiver configurations shown in Fig. 1. Nevertheless in the following the detailed description of the modeling and the sensitivity analysis is referring to one case only. The exemplary results refer to the configuration with an air stable receiver and a flat glass cover, see Fig. 1a.

Tab. 1 Overview of subscripts of individual heat transport effects according to Fig. 4

Subscript	Surface
1	Heat transfer fluid
2	Inner absorber surface
3	Outer absorber surface
6	Inner secondary mirror surface
6g	Inner glass plate surface

Subscript	Surface
7	Outer secondary mirror surface
7g	Outer glass plate surface
8	Inner casing surface
9	Outer casing surface
10/11	Ground or air / Sky

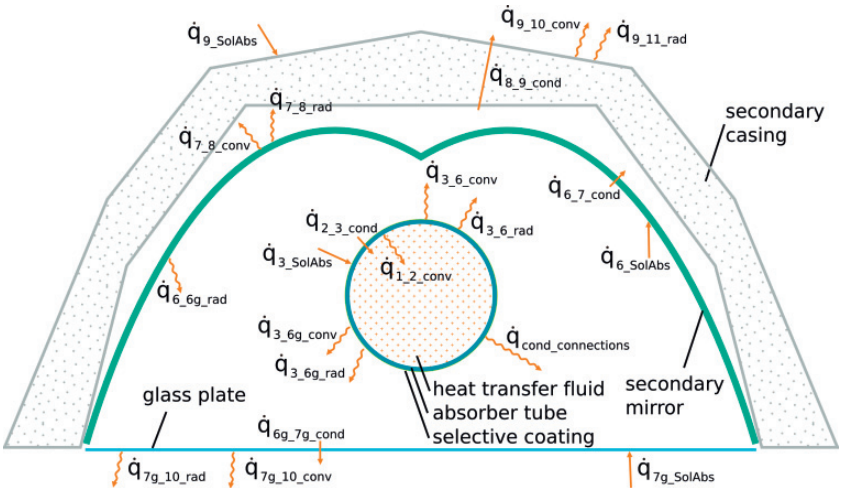

Fig. 4. Thermal balance of a Linear Fresnel Collector receiver with glass cover. The indices of the heat flows characterize the direction of the heat transport from which surface to which surface with the meanings of the indices according to Tab. 1.

In view of the aforementioned heat transfer conditions a fitted system of equations is generated, following the indices of the heat flows according to the explanations in Fig. 4 and Tab. 1. With $\dot{q}_{3\_rad}$, $\dot{q}_{6\_rad}$ and $\dot{q}_{6g\_rad}$ being the sum of all radiation reaching the designated inner surface of the receiver:

$$\dot{q}_{1\_2\_conv} = \dot{q}_{2\_3\_cond} \quad (1)$$

$$\dot{q}_{2\_3\_cond} + \dot{q}_{3\_6\_conv} + \dot{q}_{3\_6g\_conv} = \dot{q}_{3\_SolAbs} + \dot{q}_{3\_rad} \quad (2)$$

$$\dot{q}_{3\_6g\_conv} + \dot{q}_{6g\_rad} = \dot{q}_{6g\_7g\_cond} \quad (3)$$

$$\dot{q}_{6g\_7g\_cond} + \dot{q}_{7\_SolAbs} = \dot{q}_{7g\_10\_conv} + \dot{q}_{7g\_10\_rad} \quad (4)$$

$$\dot{q}_{6\_SolAbs} + \dot{q}_{3\_6\_conv} + \dot{q}_{6\_rad} = \dot{q}_{6\_7\_cond} \quad (5)$$

$$\dot{q}_{6\_7\_cond} = \dot{q}_{7\_8\_conv} + \dot{q}_{7\_8\_\_rad} \quad (6)$$

$$\dot{q}_{7\_8\_conv} + \dot{q}_{7\_8\_\_rad} = \dot{q}_{8\_9\_cond} \quad (7)$$

$$\dot{q}_{8\_9\_cond} + \dot{q}_{9\_SolAbs} = \dot{q}_{9\_10\_conv} + \dot{q}_{9\_11\_\_rad} \quad (8)$$

This system of equation is solved in an iterative process to reach a steady-state equilibrium in every node along a predefined, solar radiated receiver length in dependence of a chosen resolution. The calculation procedure is conducted by a numerical solver from the GNU scientific library [10] and being able to achieve fast calculation times of only a few seconds. The thermal resistance model underlying the set of equations is depicted in Fig. 5.

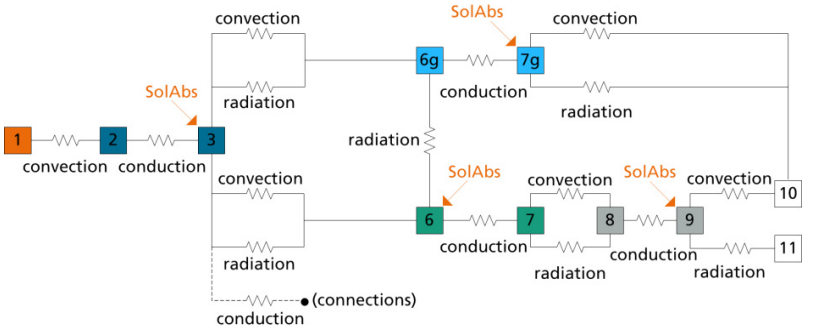

Fig. 5. Thermal resistance model of a LFC receiver with glass plate (indices according to Tab. 1)

3. Exemplary results

In previous heat loss characterization of LFC receivers [11], the effect of the absorbed radiation has not been considered in the thermal balance. With the developed models, it is possible to analyze heat loss and temperature distribution considering this effect. At the end of this section an exemplary sensitivity analysis is carried out with the simplified model, showing effects of geometry, material parameter and heat transport mechanism. The first part of the analysis in section 3.1 is constrained to the model configuration were only the heating of the absorber is considered. This is the approach which was applied up to date to LFC collector analysis. The modeling results are analyzed for the fraction of loss due to convective or radiative heat transport. In section 3.2 absorption of radiation on the secondary concentrator is taken into account. Five cases are evaluated with increasing temperature differences between absorber and secondary reflector. Finally in section 3.3 results of a sensitivity analysis are presented. During the whole analysis, we have normalized the values, in order to show the relative behavior of heat loss and its convective and radiative fraction. A verification of our models by comparison with measurement results of a receiver tested at our laboratory is currently ongoing, so far indicating the general applicability of the models.

3.1. Heat loss of a LFC receiver without considering absorbed radiation on the secondary reflector

For the calculation of the following results, measurements of an air receiver (compare configuration Fig. 1a), where only the absorber is heated and no absorption on the secondary reflector is considered, were emulated. This is a common state of the art configuration and complies with the modeling approach for parabolic trough receiver. CFD simulations were carried out for varying virtual absorber temperatures of 150 °C up to a temperature of 300 °C in steps of 50 °C, whereas for the thermal resistance model the thermal balance is calculated for steps of 0.1 °C, generating an almost continuous curve. Heat loss calculated with both models show a similar relative behavior (see Fig. 6, below). In Fig. 6 all the values have been normalized to the heat loss considering an absorber temperature of 300 °C. The results obtained from simulations show concordance with general behavior of first measurement results. Further publications will include comparison with measurement results and a thorough analysis of model and measurement uncertainties.

The models allow for analyzing the convective and radiative heat transport (see Fig. 6). For this specific case, the convective loss dominates the heat transport. We want to stress that this result is exemplary and that the radiative transport depends strongly on the emissivity of the absorber. CFD model and simplified model show a very good correlation for the convective part and small differences for the radiative part.

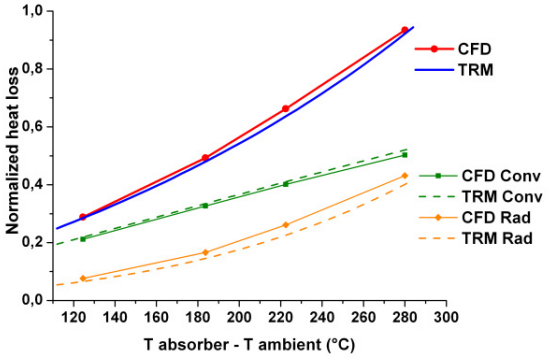

Fig. 6. Comparison of heat loss calculated with CFD model and TRM model. For both models the results for the convective heat transfer (green) and radiative heat transfer (orange) is calculated separately.

3.2. Analysis considering radiation absorbed by the secondary reflector

Fig 7a shows simulation results for the CFD model described in section 2.2, only considering the heating of the absorber. In comparison a result of our CFD simulation model combined with ray tracing, taking into account spatially resolved radiation, results in temperature peaks at the shoulder of the secondary mirror, see Fig. 7b. The peaks are located in zones exposed to high short wavelength radiative flux, reaching values even slightly higher than the absorber temperature. In case spatially resolved absorbed radiation is not considered, the temperature levels of the secondary reflector surface are clearly underestimated.

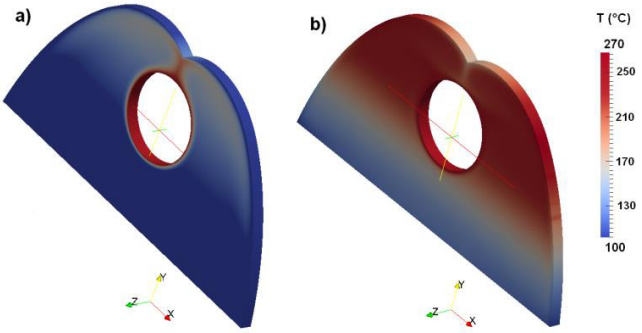

Fig. 7. Temperature field from CFD simulations . (a) Temperature field with absorber heated to a temperature of 250°C. (b) Temperature field with additional input of radiation absorbed by the secondary mirror, for normal incidence on the collector (primary mirror array) and a DNI of 800 W/ m² (similar to Figure 3 a).

In Fig. 8 a comparison of the heat loss of the receiver is shown. Take notice, that the computation of the heat loss values of Fig. 8 has been calculated for a boundary condition opposed to the simulations presented before. In the following a set of temperature profiles is given as input and the resulting heat loss is evaluated. The fixed temperature differences between absorber and mirror are set according to experience gained through ray tracing and collector measurements. Five different cases for temperature profiles on the secondary mirror are analyzed. We are not displaying the individual profiles here, but in Tab. 2 the increase in temperature difference between mean absorber temperature and mean secondary temperature is listed. The increase in temperature difference relates to a decrease of the absolute temperature on the reflector, for a constant absorber temperature of about 250°C .

Tab. 2. Difference between mean absorber and mean secondary reflector temperatures.

Case	T_{abs}- T_{sec} (°C)
1	0
2	4
3	23
4	30
5	55

The total amount of heat loss is increasing with larger temperature difference between the absorber and the secondary. The convective part of the heat loss is increasing with temperature difference, see Fig. 8a. The total heat loss of LFC receiver is overestimated if the temperature balance in the cavity is not considered, see Fig. 8b. This seems to be a reasonable result since the heat loss is here defined as the loss of useful energy related to the absorber tube and its outer temperature itself.

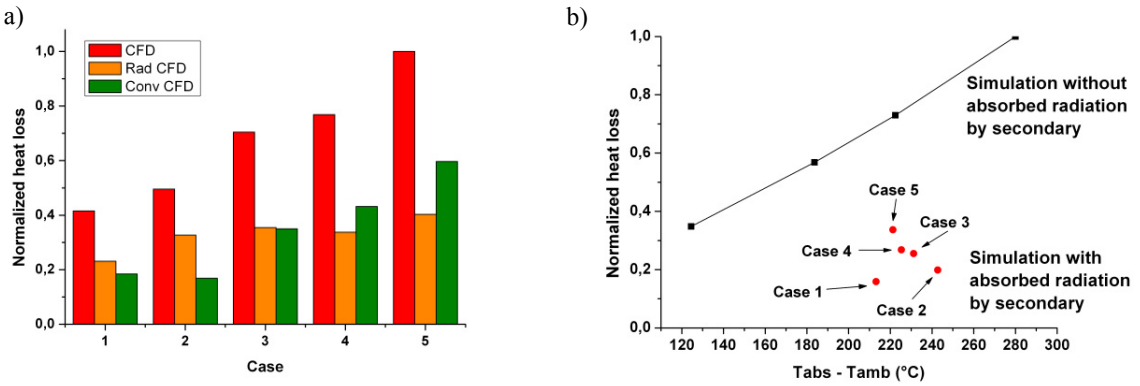

Fig. 8. (a) Heat loss results from CFD simulations. (b) Normalized values of simulated results for both cases, with and without secondary heating

3.3. Sensitivity analysis conducted with thermal resistance model

From ray tracing simulations a total absorbed radiation by the secondary mirror of 600 W/m (per meter length of collector) is estimated (see section 2.1). The calculation of this value is considering perpendicular incidence over the primary field and DNI of 1000 W/m^2. These conditions are considered as an upper limit, estimating in this way a maximum value absorbed by the secondary reflector. Given these terms, the influence of a variation of the amount of radiation absorbed by the secondary mirror is analyzed with the TRM, compare 2.3. The calculated corresponding heat loss is separated in terms of convection and radiation, see Fig. 9 In Fig. 9 all resulting values have been normalized to the maximum heat loss calculated with the input parameter of 300°C absorber temperature and the assumption of no absorbed radiation on the secondary reflector. The aim of this analysis is to show the effect resulting from a negligence of absorbed radiation on the secondary reflector. A sequential variation of optical efficiency is not considered here, but would be included in an overall optimization. As expected, the heat loss decreases with increasing absorbed radiation. For very low absorber temperatures, the secondary mirror will even become a heat source for the absorber (compare Fig. 9a where for low temperatures the heat loss becomes negative), corresponding to e.g. early morning situations. This complies with the results of the CFD simulation of the previous section and underlines the fact that the consideration of the absorbed radiation of the secondary mirror has a significant influence on the overall heat loss. Separating the overall heat loss into a radiative and a convective terms (as in Fig. 9b) shows, that especially the convection inside the cavity receiver is affected by changing absorption conditions, whereas the radiative terms do not vary much. From these results it can be deduced that a heat loss

model obly considering an absorbed radiation of 0 W/m² overestimate the heat loss of a LFC, especially for convective heat transport. This should be considered in future design optimizations of a LFC receiver.

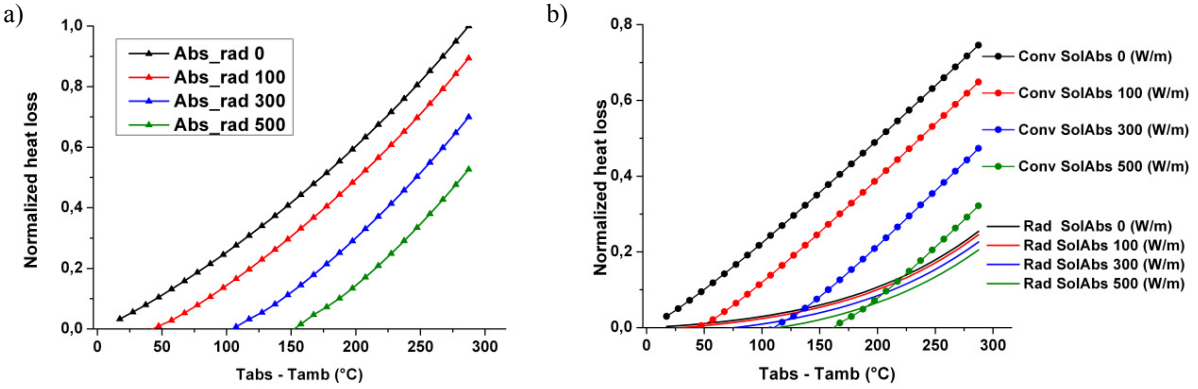

Fig. 9. (a) Heat loss for different amounts of radiation absorbed by secondary mirror (SolAbs). Values varied from no absorbed radiation up to 500 W/m. (b) Corresponding convective and radiative heat transfer fractions. All values normalised to the maximum heat loss for Tabs=300°C SolAbs=0.

Relevant design parameters to vary for a thermal optimization are the absorber diameter, distance to the secondary mirror, emittance and reflectance of the surfaces. In the following the influence of the absorber diameter and emittance is evaluated. The parameter variation depicts the effect of changing the geometry and physical properties of its components from a thermal point of view. Changing these parameters will result in a variation on the optical efficiency as well, to be considered in the overall optimization, but this effect is not considered here.

The variation of absorber tube diameter shows, as expected, an increase of heat loss with increasing surface area and increasing temperature (compare Fig. 10). The results of this sensitivity study once again comply with the general conclusion, that heat loss decreases significantly by considering radiation absorbed by the secondary mirror. Analyzing into more detail the effect of decreasing absorber diameter, one comes to the conclusion, that with standard heat loss models (characterized by an amount of absorbed radiation of 0 W/m) the effect of a smaller absorber size on the overall heat loss may be overestimated.

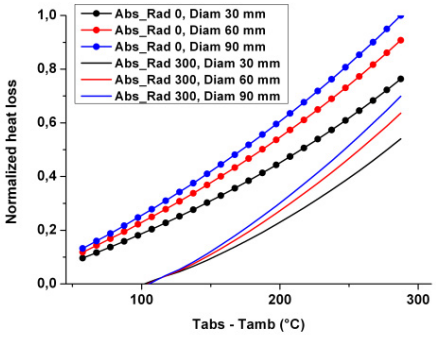

Fig. 10. Impact of variation of absorber diameter (30/60/90 mm) on heat loss for the case of no absorbed radiation on the secondary reflector (0 W/m) and for the case of a mean absorbed radiation of 300 W/m.

Additionally, the effect of varying emittance values of the absorber has been analyzed with the new simplified model. Two different emittance ranges have been considered. The first option (abbreviated as Emiss 1) correlates to comparatively low emittance values in the range of 6% at 150 °C and 8% at 300 °C for the absorber coating. The second emittance value (abbreviated as Emiss 2) correlates to an emittance in the range of 12% at 150 °C and 16%

at 300 °C. As expected, Fig. 11 depicts the fact, that a lower emittance (with Emiss 1) implicates lower heat loss in comparison with a higher emissivity of the absorber (with Emiss 2). Taking a deeper look on the heat loss data the influence of emittance reduction can be evaluated. Optimizing the absorber properties from high emittances to lower ones (from Emiss 2 to Emiss 1), without considering absorption of the secondary mirror (SolAbs = 0 W/m), heat loss can be decreased up to around 16%. Evaluating the effect of reduced emittance by considering the absorption of the secondary mirror (SolAbs = 300 W/m) the heat loss decreases around 21%. As a consequence with the standard PTC model the effect of an emittance-optimized absorber surface due to lower emittance values is underestimated. This confirms the use of a more elaborated heat loss model for LFC.

Fig. 11b shows the separation of the overall heat loss into a convective and radiative part for the two emittances. Considering the absorption of the secondary mirror, the convection decreases whereas the radiative term changes just slightly (compare all black lines). Additionally, Fig. 11b demonstrates a second effect: reducing the emittance (from Emiss 2 to Emiss 1) has nearly no influence on the convective part (compare red and black line with circles), but a high impact on the radiation within the cavity of the receiver (see red and black continuous line). The same effect can also be identified considering absorption in the secondary (compare red and black line with rectangles for convection and red and black dashed line for radiation). This means, that the convection within the receiver depends strongly of the amount of absorbed energy of the secondary mirror, whereas the radiation mainly depends on the emittance of the absorber. This correlation can be regarded as valuable information to be considered in future design optimization of the cavity of a LFC receiver.

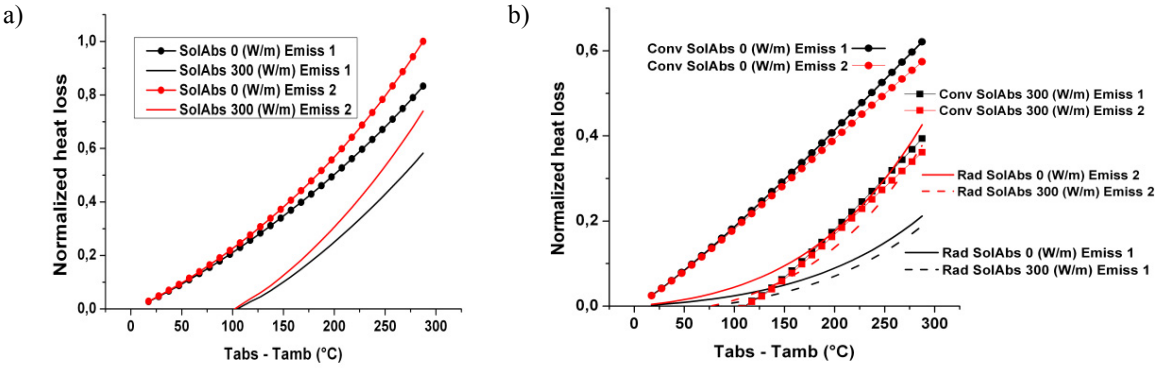

Fig. 11. (a) Heat loss for two different absorber emittance, Emiss 1 being smaller than Emiss 2. (b) Seperation of radiative and convective terms of the overall heat loss in dependence of the amount of absorbed radiation (Solabs = 0 or 300 W/m) and emissivity values (Emiss 1 and Emiss2).

4. Conclusion

In the present work two methods to calculate heat loss and temperature distribution of LFC receivers are presented. The detailed model is applying a combination of ray tracing and CFD. It allows for the prediction of both temperatures in the receiver cavity and heat loss. The advantage is a detailed spatial resolution of convection and temperature field. A disadvantage is the calculation time of the detailed numerical model. The modeling results highlight the underestimation of temperatures at the secondary reflector in previous investigations. An experimental validation of the thermal models is currently ongoing. The TRM model allows fast calculations in order to analyze general behavior for a variation of material and geometrical parameters. The model results for heat loss calculation are in good compliance with the results of the more detailed CFD model. A simplification of the model is the assumption of a mean temperature on the secondary mirror and a constant amount of absorbed energy. Yet, the model is also applicable to configurations with a circular glass tube, although the results in this paper focus on a receiver with an air stable absorber coating and a flat glass cover. For this configuration (see Figure 1a) and an absorber temperature of about 250°C the presented results and preliminary measurements indicate that it is important to consider absorption of concentrated solar radiation on the mirrors of the LFC receiver. The sensitivity

analysis shows that the effect of absorbed radiation may be larger than the effect of material parameters such as the emissivity or the diameter of the absorber. The reason for this is an overestimation of the heat loss of the receiver without considering the secondary mirror and its temperatures. Energy absorption by surfaces can be treated as a heat generation phenomena and as such, it has an effect on the temperatures. Therefore considering this effect in the thermal balance is significant. For the identification of performance parameters from thermal testing of a LFC, the disregard of the absorption by the secondary reflector might lead to a small overestimation of the optical efficiency.

Furthermore, we want to emphasize that the absorbed radiation, varied in the sensitivity analysis, would depend not only on the DNI and sun position, but also on the collector geometry, tracking strategy and the optical properties of the interacting surfaces. As a consequence the heat loss of a cavity LFC receiver does not only depend on the absorber temperature. The order of magnitude of these effects are still under investigation and in our ongoing research the effects on yield simulations will be quantified, aiming at a more detailed performance model for LFCs.

References

[1] Forristall R. Heat Transfer Analysis and Modeling of a Parabolic Trough Solar Receiver Implemented in Engineering Equation Solver, Technical Report, National Renewable Energy Laboratory NREL.

[2] Mertins M. Technische und wirtschaftliche Analyse von horizontalen Fresnel-Kollektoren. Dissertation an der Universität Karlsruhe; Fakultät für Maschinenbau.2008

[3] Branke R, Heimsath A. Raytrace 3D-Power Tower- A novel optical model for central receiver systems, 16th Solar Paces Conference. Perpignan.2010

[4] Helmers H, Thor W, Schmidt T, Van Rooyen DW. An optical analysis of deviations in a CPV central receiver system with a flux homogenizer. Applied Optics, 2013. 52(13): pp. 2974-84. DOI: 10.1364/AO.52.002974

[5] Morin G, Platzer W, Strelow M, Leithner R. Techno-Economic System Simulation and Optimization of Solar Thermal Power Plants. 14th Solar Paces Conference. Las Vegas. 2008.

[6] Modest M, Radiative Heat Transfer, 2002, Second Edition, Academic Press.

[7] Lewis R, Nithiarasu P, Seetharamu K, Fundamentals of the Finite Element Method for Heat and Fluid Flow, 2004, John Wiley & Sons.

[8] VDI Heat Atlas. 2002, Second Edition, Springer, Berlin Heidelberg

[9] View3D, http://view3d.sourceforge.net (accessed 04.10.2011)

[10] Gnu scientific library, http://www.gnu.org/software/gsl/ (accessed 15.02.2013)

[11] Bernhard, R. LaLaing, J. Kistner, R. Eck, M. Eickhoff, M. Feldhoff, F. Heimsath, A. Hülsey, H. Morin, G. Linear Fresnel Collector Demonstration at the PSA- Operation and investigation. 15th Solar Paces Conference. Berlin.2009